Skyrme Hartree-Fock calculations for the α-decay Q values of superheavy nuclei

S. Typel* and B. A. Brown
Department of Physics and Astronomy and National Superconducting Cyclotron Laboratory, Michigan State University, East Lansing, Michigan 48824-1321
(Received 15 November 2002; published 24 March 2003)

Hartree-Fock calculations with the SKX Skyrme interaction are carried out to obtain α-decay Q values for deformed nuclei above ^{208}Pb assuming axial symmetry. The results for even-even nuclei are compared with the experiment and with the previous calculations. Predictions are made for α-decay Q values and half-lives of even-even superheavy nuclei. The results are also compared for the recently discovered odd-even chain starting at $Z=112$ and $N=165$.

DOI: 10.1103/PhysRevC.67.034313 PACS number(s): 23.60.+e, 21.10.Dr, 21.60.Jz, 27.90.+b

I. INTRODUCTION

The existence and decay properties of superheavy nuclei are one of the most fundamental problems in nuclear physics [1,2]. There are now new data that confirm the existence of $Z=111$ and 112, and their connection to lighter decay chains [3]. The first data for $Z=114$ and $Z=116$ also exist [4], with suggested $A=288$ and $A=292$, respectively, but the A values are not certain since the connection to lighter nuclei is not known. Theoretical models for superheavy nuclei have evolved from the macroscopic-microscopic models such as the finite-range droplet model with shell corrections [5] to the fully microscopic deformed Hartree-Fock (HF) models such as those presented in Refs. [6,7]. In addition to their intrinsic many-body nuclear structure importance, theoretical models for the prediction of the decay properties of the superheavy nuclei are important when designing the experiments since the techniques used will depend on the half-life and decay mode.

In this paper, we present a new set of Hartree-Fock results for α-decay Q values of superheavy nuclei. A global formula is used to calculate the half-lives. Our calculations are based upon a different computational program for solving the axial-symmetric HF equations and the Skyrme interaction SKX [8]. The reason for exploring results with another Skryme interaction beyond those used previously in Refs. [6,7] is that the α-decay Q-value systematics are sensitive to the spherical and deformed shell effects, which depend upon the underlying parameters of the Hamiltonians. There are several modern Skyrme parameter sets available, each of them determined with a different weighting and emphasis on the existing nuclear structure properties.

The SLy4 parameters [9] used in Ref. [6] and the MSk7 [7] parameters take into account the overall spacing of the single-particle states, such as those in ^{208}Pb. (In particular, it is common to constrain the Skyrme parameters to give an effective mass of unity, which is required by the observed level spacing.) However, the SKX interaction [8] explicitly incorporates most of the observed single-particle levels in ^{208}Pb into the dataset that was used to determine the parameter values. Another difference between the three Skyrme parametrizations is the treatment of the Coulomb exchange contribution. In the SKX force this term is neglected, but most of its effect on the binding energies is effectively included in the terms for the central potential by a refit of the Skyrme parameters. Thus Q values obtained with the SKXce Hamiltonian [8] (which includes the Coulomb exchange interaction) are essentially the same as those obtained with SKX.

The single-particle energies for some proton and neutron particle states above the Fermi surface in ^{208}Pb are compared in Table I. They were calculated with the parameters of the three forces with our code. Our results for the SLy4 force agree very well with the level energies as shown in Fig. 5 of Ref. [9]. All of the calculations have some disagreement with the experiment; however, SKX has the best overall agreement with the experiment. It is important to explore the model dependences of the HF results for the binding energies of nuclei above ^{208}Pb.

In Sec. II, we will briefly discuss the computational method for the binding energies and single-particle spectra for axial-symmetric nuclei in the HF approximation. In Sec. III, the results for α-decay Q values and lifetimes will be presented and discussed. The region of the chart of nuclides covered by our calculations is shown in Fig. 1. This includes the region just above ^{208}Pb where the α-decay Q values are measured, and extends up to the assumed spherical magic

TABLE I. Single-particle energies for states in ^{208}Pb and the rms difference between the experiment and the theory.

	Single-particle energy (MeV)			
Orbit	Experiment	SKX	SLy4	MSk7
$\pi 1h_{9/2}$	−3.80	−4.26	−3.82	−3.47
$\pi 2f_{7/2}$	−2.90	−2.83	−2.93	−3.19
$\pi 1i_{13/2}$	−2.29	−2.18	−1.46	−2.62
$\pi 2f_{5/2}$	−0.98	−0.70	−0.37	−0.93
$\nu 2g_{9/2}$	−3.94	−3.46	−3.14	−4.05
$\nu 1i_{11/2}$	−3.16	−2.81	−1.57	−2.02
$\nu 1j_{15/2}$	−2.16	−1.97	−0.64	−2.53
$\nu 2g_{7/2}$	−1.45	−1.00	0.08	−0.97
rms		0.34	1.05	0.51

*Present address: Gesellschaft für Schwerionenforschung mbH, Planckstraße 1, 64291 Darmstadt, Germany.

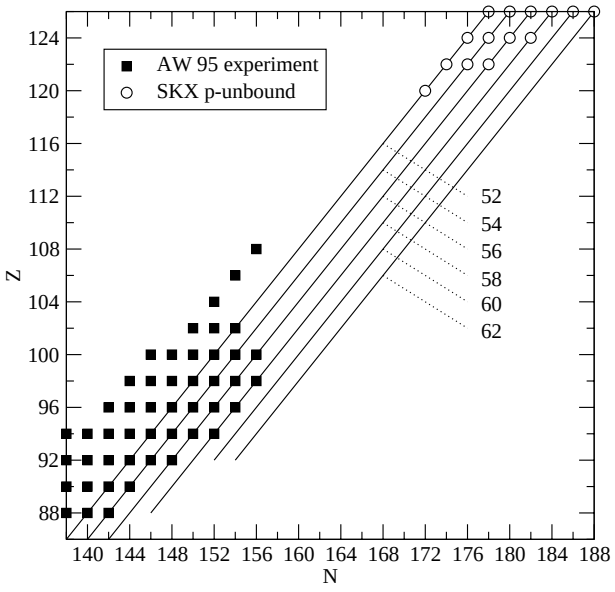

FIG. 1. Chart of the nuclides for even-even nuclei with $N \geqslant 138$ and $Z \geqslant 86$. Solid squares denote nuclei with the experimentally known masses. Nuclei discussed in this paper are located on the solid lines with constant $N-Z$ (indicated by the numbers). Open circles indicate proton-unbound nuclei in the SKX parametrization.

numbers of $Z=126$ and $N=184$ for the superheavy predictions.

II. METHOD OF CALCULATION

There are several methods available for solving the Schrödinger equation for the single-particle wave functions ϕ_i in a Skyrme-type potential with axial symmetry. Often a cylindrical coordinate system is chosen and the wave functions are expanded in a deformed harmonic oscillator basis with carefully adjusted oscillator strengths. Then the Hamiltonian is diagonalized in an appropriately truncated space of basis states. Here, we solve the Schrödinger equation for ϕ_i in coordinate space with a spherical basis for the angular part of the wave function. In this approach, there is a smooth transition to the case of spherical nuclei where the wave function simplifies considerably.

The single-particle wave functions of protons ($q=+1$) and neutrons ($q=-1$) in a deformed nucleus with axial symmetry are specified by three quantum numbers: the parity $\pi=\pm 1$, the principal quantum number $n=1,2,\ldots$, and the projection of the total angular momentum on the symmetry axis $\Omega=\pm\frac{1}{2},\pm\frac{3}{2},\ldots$. We expand the wave functions in coordinate space,

$$\phi_{q\pi n\Omega}(\vec{r})=\frac{1}{r}\sum_{\kappa} f_{q\pi n\kappa\Omega}(r)\mathcal{Y}_{\kappa\Omega}(\hat{r}), \tag{1}$$

with the radial wave functions $f_{q\pi n\kappa\Omega}(r)$ and vector spherical harmonics

$$\mathcal{Y}_{\kappa\Omega}(\hat{r})=\sum_{m\nu} (lms\nu|j\Omega)Y_{lm}(\hat{r})\chi_{s\nu}, \tag{2}$$

which are obtained by coupling the orbital angular momentum l of the spherical harmonics Y_{lm} and the spin $s=\frac{1}{2}$ of the spinors $\chi_{s\nu}$ to the total angular momentum j. The index κ of the vector spherical harmonic of Eq. (2) specifies $j=|\kappa|-\frac{1}{2}$, with $l=\kappa-1$ for $\kappa>0$ and $l=-\kappa$ for $\kappa<0$. The sum in Eq. (1) runs over all κ with $|\kappa|\geqslant|\Omega|+\frac{1}{2}$, where $\kappa\in\{1,-2,3,-4,\ldots\}$ for positive parity states and $\kappa\in\{-1,2,-3,4,\ldots\}$ for negative parity states. The Schrödinger equation for $\phi_{q\pi n\Omega}$ leads to a set of coupled differential equation for the radial wave functions $f_{q\pi n\kappa\Omega}(r)$ for all allowed κ. In the actual calculation, only the contributions with $|\Omega|+\frac{1}{2}\leqslant|\kappa|\leqslant|\Omega|+\frac{25}{2}$ are considered. The radial wave functions are discretized on a grid with a step size of $h=0.2$ fm inside an interval $[0,R]$ with maximum radius $R=(1.25A^{1/3}+12)$ fm for a nucleus with A nucleons. Derivatives are represented by five-point formulas.

Particle densities ϱ_q, kinetic energy densities τ_q, and spin-current densities $\vec{J}_q$ appearing in the Skyrme Hartree-Fock potentials and the energy density are easily calculated from the single-particle wave functions $\phi_{q\pi n\Omega}$. For example, proton and neutron single-particle densities are given by the multipole expansion

$$\varrho_q(\vec{r})=\sum_{L} \varrho_{qL}(r)Y_{L0}(\hat{r}), \tag{3}$$

where

$$\varrho_{qL}(r)=\sum_{\pi n\Omega}\frac{w_{q\pi n\Omega}}{r^2}\sum_{\kappa\kappa'} C^{L\Omega}_{\kappa\kappa'}f^{*}_{q\pi n\kappa\Omega}f_{q\pi n\kappa'\Omega} \tag{4}$$

with coefficients

$$C^{L\Omega}_{\kappa\kappa'}=\int d\Omega\mathcal{Y}^{\dagger}_{\kappa\Omega}Y_{L0}\mathcal{Y}_{\kappa'\Omega}. \tag{5}$$

The occupation probabilities $w_{q\pi n\Omega}$ in each state are determined by the BCS calculation. Only even values of L appear in the sum of Eq. (3) and contributions $0\leqslant L\leqslant 10$ are considered in the calculation. The nonradial contributions of the spin-current density are neglected in the calculation.

The binding energy of nucleus with A nucleons and Z protons in its ground state is calculated from

$$BE(A,Z)=-(E_{mf}+E_{pair}-E_{cm}-E_{rot}), \tag{6}$$

with the mean-field contribution

$$E_{mf}=\int d^3rH(\vec{r}), \tag{7}$$

which is obtained by integrating the Skyrme Hartree-Fock energy density $H(\vec{r})$ over the spatial coordinates. The pairing energy in the BCS approach is given by

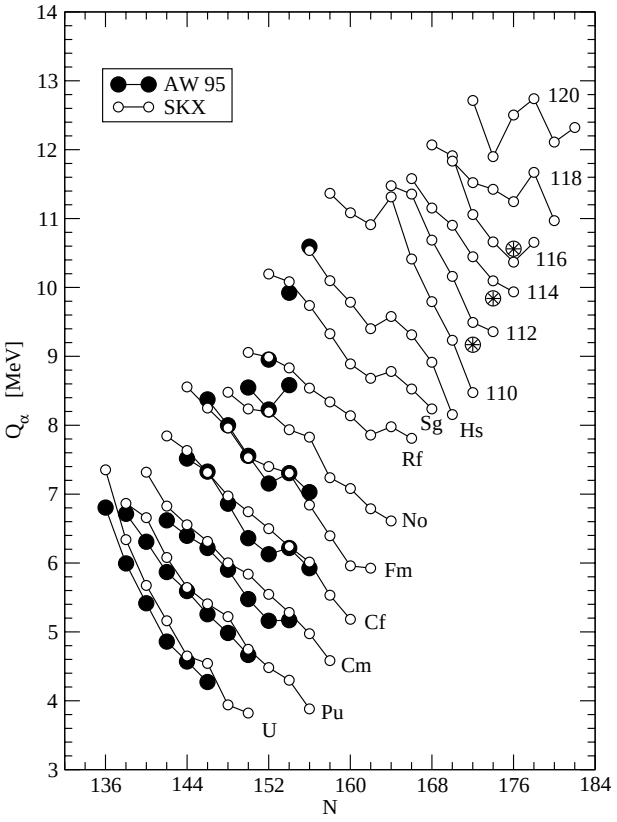

FIG. 2. Q value for α decay as a function of the neutron number N connected by lines for the given Z values. The experimental values are shown by the solid circles. The results from the SKX deformed HF calculations are given by the open circles.

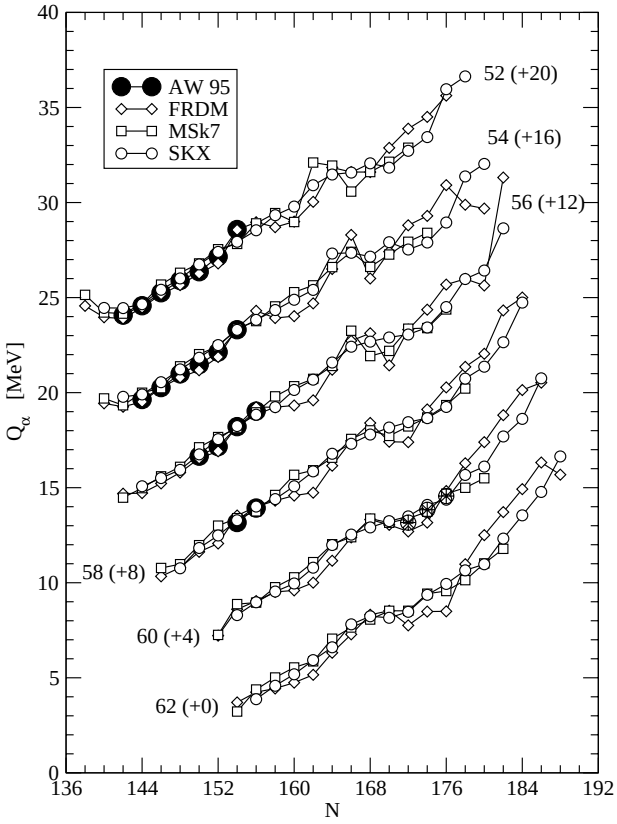

FIG. 3. Q value for α decay as a function of the neutron number N for even-even nuclei located on the solid lines of Fig. 1. Predictions from the finite-range droplet model (open diamonds represent FRDM), and two Skyrme Hartree-Fock parametrizations (open squares represent MSk7 and open circles represent SKX) are compared with the experimental data (solid circles). Different decay chains with the same value of $N-Z$ (indicated by the numbers) are connected by solid lines and shifted vertically by the amount (in MeV) shown in parentheses.

$$E_{pair} = -\sum_q \frac{G_q}{4}\left(\sum_{\pi n\Omega} \sqrt{w_{q\pi n\Omega}(1-w_{q\pi n\Omega})}\right)^2. \quad (8)$$

The pairing strength is $G_{+1}=1.9/\sqrt{A}$ MeV for protons and $G_{-1}=1.2/\sqrt{A}$ MeV for neutrons, respectively. These values were obtained from a fit to the experimental pairing gaps of $N=146$ isotones and $Z=92$ isotopes. Only bound states are considered in the determination of the occupation probabilities $w_{q\pi n\Omega}$ in the BCS calculation. The correction for the center-of-mass motion

$$E_{\text{c.m.}} = \frac{3}{4}(45A^{-1/3} - 25A^{-2/3}) \ \text{MeV} \quad (9)$$

is the same harmonic oscillator approximation as for spherical nuclei in the SKX parametrization. The rotational correction is approximated by

$$E_{rot} = \frac{\langle\psi|J_x^2|\psi\rangle}{2\mathcal{I}_x}, \quad (10)$$

where ψ is the many-body wave function of the nucleus in the BCS ground state. The moment of inertia $\mathcal{I}_x$ for the rotation around the x axis is calculated in the cranking model.

III. RESULTS

The deformed HF calculations give the binding energies for the nuclei above ^{208}Pb. From these we calculate the α-decay Q value, $Q_\alpha = BE(A-4,Z-2) + BE(4,2) - BE(A,Z)$, where the experimental value of $BE(4,2) = 28.30$ MeV is used for the α particle. The results for α-decay Q values for even-even nuclei are shown in Fig. 2. The purpose is to compare with the measured Q values as well as to compare with the results based on the SLy4 interaction shown in Fig. 1 of Ref. [6]. Comparison of the two figures shows that the results for SLy4 and SKX are remarkably similar, even though they are based upon Skyrme parameter sets that are determined completely independently. Both show good overall agreement with the experimental Q values [10] to within a rms deviation of a few hundred keV, with the exception of a dip in the experimental Q values around $N=152$, which is not present in the theory. The largest deviation for SKX is for the Q value for ^{256}No at $N=154$. We also show in Fig. 2 the comparison with the experimental Q_α values from the suggested placement of the

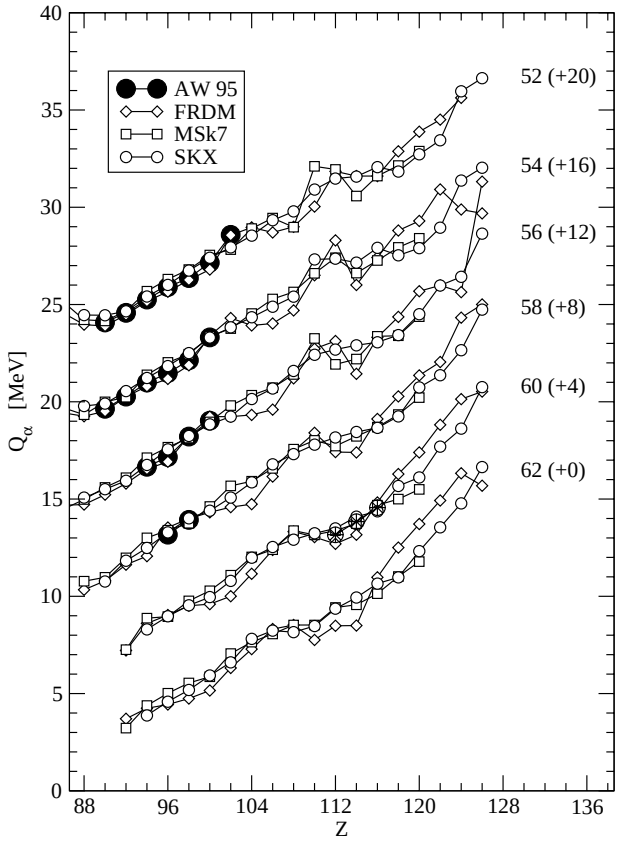

FIG. 4. Same as Fig. 3 as a function of *Z*.

$Z=116$–114–112 decay chain [4]. These also agree well with the theory.

Further results are shown in Fig. 3 as a function of neutron number and in Fig. 4 as a function of proton number. The points are connected in these figures for a given $N-Z$ value in order to emphasize how the *Q* values change in a given decay chain. Comparisons are made to the finite-range droplet model (FRDM) [5] and to the deformed HF-BCS calculations based on the MSk7 Skyrme interaction. The *Q* values for the MSk7 interaction were calculated from the binding energies as given in the table of Ref. [7]. The results for SKX and MSk7 are very similar even for the extrapolation to large *N* and *Z*. The FRDM results are similar to the HF in the region where data are available, but become more different for the extrapolation to heavier nuclei.

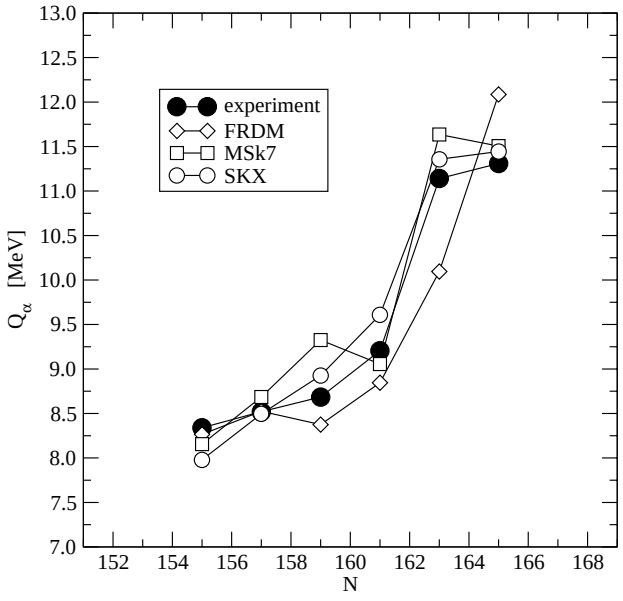

FIG. 5. Same as Fig. 3 but for the nuclei with $N-Z=53$.

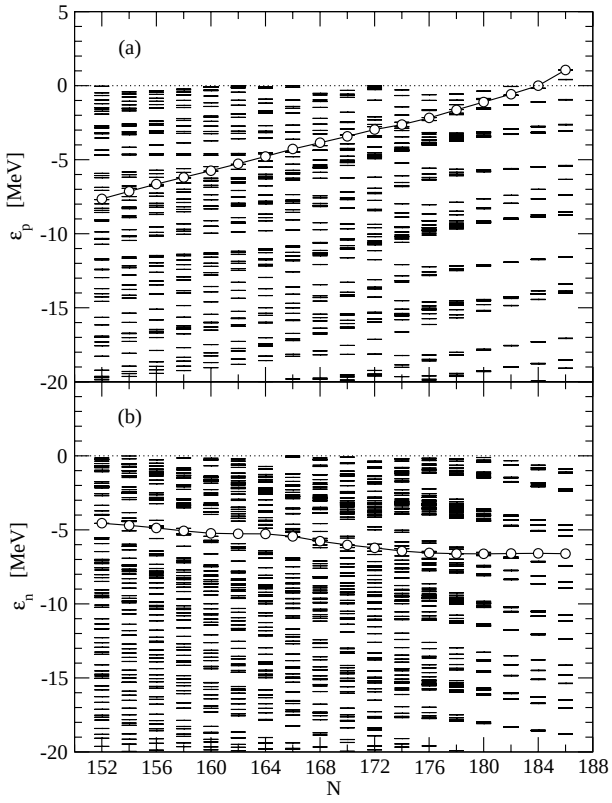

FIG. 6. Single-particle energies of protons (a) and neutrons (b) above -20 MeV in even-even nuclei with $N-Z=60$ in the Skyrme Hartree-Fock calculation with the SKX parametrization. The Fermi energies of protons and neutrons are denoted by open circles.

Much of the data for the superheavy nuclei are for odd-even decay chains. These are more difficult to calculate and compare with the experiment, since the deformed level density is high and the observed nuclei may be in isomeric states. These must be considered carefully. For this paper, we compare with the *Q* values observed for the recently confirmed decay chain for $N-Z=53$ starting at $^{277}112$ in Fig. 5. In the calculation we assume that the nucleus is in its lowest energy deformed single-particle state. The results are also compared to the FRDM and MSk7 models. As in Figs. 3 and 4, the SKX and MSk7 results are close to each other and both are close to the experiment, with perhaps SKX being in best agreement with the experiment. The FRDM results do not agree as well in detail with the experiment. In the deformed HF, the jump in *Q* value between $N=161$ and $N=163$ observed in Fig. 5 comes from a deformed shell gap at

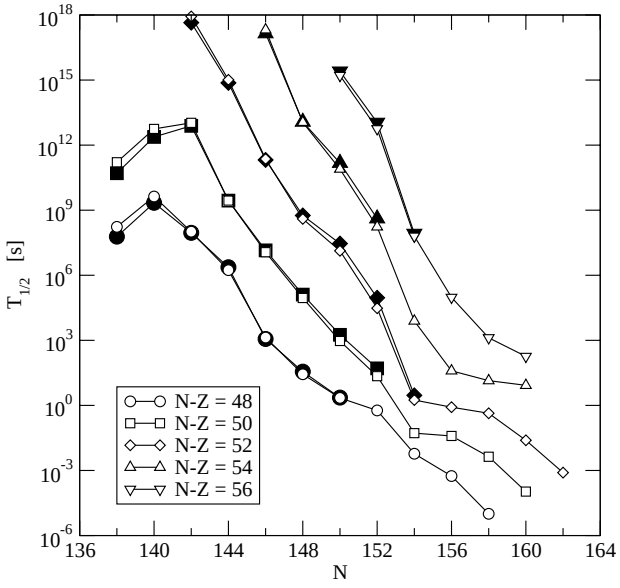

FIG. 7. Half-lives of even-even nuclei as a function of the neutron number N. Open symbols indicate half-lives calculated with Eq. (4) with the experimentally measured Q_α values or with Q_α values from the Audi-Wapstra mass extrapolation. Solid symbols denote the experimental half-lives. Decay chains with constant $N-Z$ value are connected by solid lines.

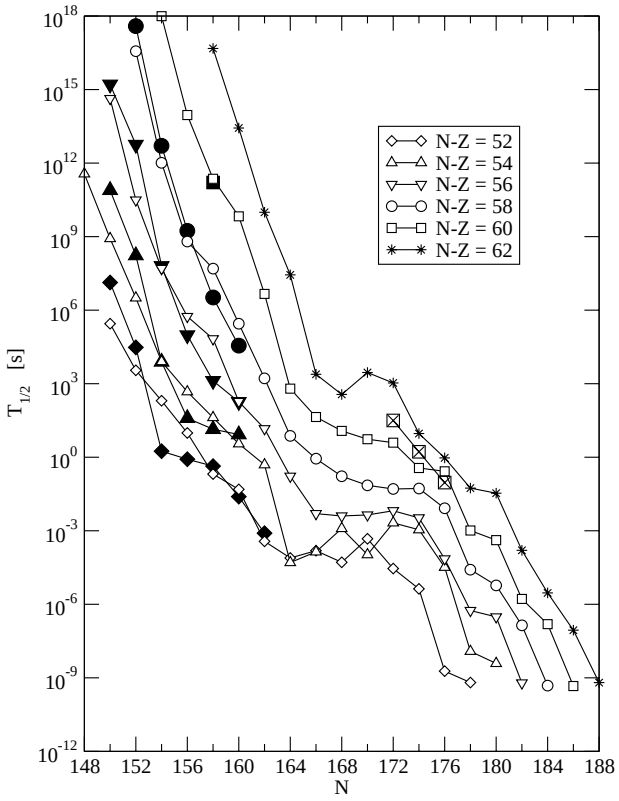

FIG. 8. Half-lives of even-even nuclei as a function of the neutron number N. Open (solid) symbols indicate half-lives calculated with Q_α values from the SKX parametrization (experiment). Decay chains with constant $N-Z$ value are connected by solid lines. The experimental half-lives from the suggested placement of the $^{292}116$ decay chain are shown by the cross-filled boxes.

$N=162$ and $Z=108$. These deformed gaps are also found with the SLy4 interaction [6]. We note that the semiempirical shell-model mass approach [11] cannot and does not take into account these deformed shell gaps and cannot reproduce any of the fine structures in the Q-value systematics.

The distribution of the single-particle energies for protons and neutrons is shown in Fig. 6 as a function of the neutron number N in even-even nuclei for the $N-Z=60$ decay chain. Nuclei with small N are well deformed and become more and more spherical with increasing N. Proton and neutron shell gaps are readily seen in both spherical and deformed nuclei. The proton Fermi energy increases smoothly with increasing N and becomes positive for the nucleus with $N=188$, which is predicted to be proton unbound in the SKX parametrization. The neutron Fermi energy decreases only slightly with increasing N. It crosses the well-defined shell gap at $N=162$, which was mentioned above.

The α-decay half-life is important for determining how the α decay of superheavy nuclei competes with fission. The extrapolated half-lives are also important for choosing the type of the experimental techniques used for their identification. The main theoretical uncertainty for the calculation of the assumed $L=0$ decays of even-even nuclei is in the α-decay Q value. To calculate the half-lives we use the empirical result obtained in Ref. [12],

$$\log_{10}[T_{1/2}/\mathrm{s}]=9.54(Z-2)^{0.6}/\sqrt{Q_\alpha/\mathrm{MeV}}-51.37. \quad (11)$$

In Fig. 7 we show the half-life calculated from Eq. (11) and from the experimental Q values [10]. The results are compared to the experimental half-lives. The excellent agreement between the experiment and the theory shows that preformation and decay systematics implied by Eq. (11) are adequate for a determination of the α-decay half-life to within about a factor of three.

The predictions for the half-lives of heavier nuclei based upon the theoretical Q_α values from our SKX calculation results are shown in Fig. 8. The agreement with the experiment is satisfactory except with near $N=152$ where the kink in the experimental half-lives is not reproduced by the theory. The experimental half-lives for the suggested placement of the $Z=116$ decay chain [4] are also in reasonable agreement with the theory. One observes an island of relative stability starting at $N=164$ where the half-lives for $Z\approx 53$ remain at the msec level or longer until $N\approx 174$ where they start to become shorter.

IV. SUMMARY

We have presented a new calculation for the α-decay Q values for superheavy nuclei based upon deformed Hartree-Fock calculations with the SKX Skyrme interaction. A different computational method is used to carry out axially symmetric deformed calculations. An agreement with the ex-

perimental data including the recently observed $Z=112$, $Z=114$, and $Z=116$ decays is obtained at the rms level of a few hundred keV. Deformed shell gaps at $N=162$ and $Z=108$ lead to jumps in the Q values, which are consistent with the experiment. The Q values have been used to calculate α-decay half-lives that are in reasonable agreement with the experiment. Predictions for the Q values and half-lives up to the proton drip line at $N=184$ and $Z=126$ are made.

ACKNOWLEDGMENT

This work was supported by U.S. National Science Foundation Grant No. PHY-0070911.

[1] P. Armbruster, Annu. Rev. Nucl. Part. Sci. **50**, 411 (2000).
[2] S. Hofmann and G. Münzenberg, Rev. Mod. Phys. **72**, 733 (2000).
[3] S. Hofmann *et al.*, Eur. Phys. J. A **14**, 147 (2002).
[4] Yu. Ts. Oganessian *et al.*, Phys. Rev. C **63**, 011301(R) (2001).
[5] P. Möller, J.R. Nix, W.D. Myers, and W.J. Swiatecki, At. Data Nucl. Data Tables **59**, 185 (1995).
[6] S. Cwiok, W. Nazarewicz, and P.H. Heenen, Phys. Rev. Lett. **83**, 1108 (1999).
[7] S. Goriely, F. Tondeur, and J.M. Pearson, At. Data Nucl. Data Tables **77**, 311 (2001).
[8] B.A. Brown, Phys. Rev. C **58**, 220 (1998).
[9] E. Chabanat, P. Bonche, P. Haensel, J. Meyer, and R. Schaeffer, Nucl. Phys. **A635**, 231 (1998); **A643**, 441 (1998).
[10] G. Audi and A.H. Wapstra, Nucl. Phys. **A595**, 409 (1995).
[11] S. Liran, A. Marinov, and N. Zeldes, Phys. Rev. C **66**, 024303 (2002).
[12] B.A. Brown, Phys. Rev. C **46**, 811 (1992).